Cellular/Molecular

KChIPs and Kv4 α Subunits as Integral Components of A-Type Potassium Channels in Mammalian Brain

Kenneth J. Rhodes,[1] Karen I. Carroll,[1] M. Amy Sung,[1] Lisa C. Doliveira,[1] Michael M. Monaghan,[1] Sharon L. Burke,[1] Brian W. Strassle,[1] Lynn Buchwalder,[2] Milena Menegola,[4] Jie Cao,[3] W. Frank An,[3] and James S. Trimmer[2,4]

[1]Neuroscience, Wyeth Discovery Research, Princeton, New Jersey 08543, [2]Department of Biochemistry and Cell Biology, State University of New York, Stony Brook, New York 11794, [3]Millennium Pharmaceuticals, Cambridge, Massachusetts 02139, and [4]Department of Pharmacology, School of Medicine, University of California, Davis, California 95616

Voltage-gated potassium (Kv) channels from the Kv4, or *Shal*-related, gene family underlie a major component of the A-type potassium current in mammalian central neurons. We recently identified a family of calcium-binding proteins, termed KChIPs (Kv channel interacting proteins), that bind to the cytoplasmic N termini of Kv4 family α subunits and modulate their surface density, inactivation kinetics, and rate of recovery from inactivation (An et al., 2000). Here, we used single and double-label immunohistochemistry, together with circumscribed lesions and coimmunoprecipitation analyses, to examine the regional and subcellular distribution of KChIPs1–4 and Kv4 family α subunits in adult rat brain. Immunohistochemical staining using KChIP-specific monoclonal antibodies revealed that the KChIP polypeptides are concentrated in neuronal somata and dendrites where their cellular and subcellular distribution overlaps, in an isoform-specific manner, with that of Kv4.2 and Kv4.3. For example, immunoreactivity for KChIP1 and Kv4.3 is concentrated in the somata and dendrites of hippocampal, striatal, and neocortical interneurons. Immunoreactivity for KChIP2, KChIP4, and Kv4.2 is concentrated in the apical and basal dendrites of hippocampal and neocortical pyramidal cells. Double-label immunofluorescence labeling revealed that throughout the forebrain, KChIP2 and KChIP4 are frequently colocalized with Kv4.2, whereas in cortical, hippocampal, and striatal interneurons, KChIP1 is frequently colocalized with Kv4.3. Coimmunoprecipitation analyses confirmed that all KChIPs coassociate with Kv4 α subunits in brain membranes, indicating that KChIPs 1–4 are integral components of native A-type Kv channel complexes and are likely to play a major role as modulators of somatodendritic excitability.

Key words: **long-term potentiation; synaptic plasticity; A current; Shal; hippocampus; Alzheimer's disease**

Introduction

In mammalian central neurons, certain rapidly inactivating, or A-type, voltage-gated potassium (Kv) currents are concentrated in somatodendritic membranes (Sheng et al., 1992; Bekkers, 2000a,b; Korngreen and Sakmann, 2000) where they shape postsynaptic responses to excitatory input (Johnston et al., 2000, 2003; Storm, 2000), regulate amplitude and duration of back-propagating action potentials (Hoffman et al., 1997), and modulate dendritic excitability in response to second messenger activation (Nakamura et al., 1997; Hoffman and Johnston, 1998; Holmqvist et al., 2001) and long-term potentiation (Frick et al., 2004). Immunohistochemical analyses (Sheng et al., 1992; Maletic-Savatic et al., 1995; Tsaur et al., 1997; Varga et al., 2000; for review, see Trimmer and Rhodes, 2004), pharmacological sensitivity (Wu and Barish, 1992; Holmqvist et al., 2001), and electrophysiological characteristics (Serôdio et al., 1994, 1996; Serôdio and Rudy, 1998) suggest that a major component of the somatodendritic A-type Kv current is formed by α subunits from the *Shal* or Kv4 family (Gutman et al., 2003). However, A-type currents from Kv4 α subunits expressed in heterologous cells and neurons differ. That coexpression of Kv4 α subunits with brain mRNA in heterologous cells gives rise to A-type currents with a more "native" phenotype (Rudy et al., 1988; Chabala et al., 1993; Serôdio et al., 1994) prompted our search for accessory Kv4 channel subunits.

We used the cytoplasmic N terminus of Kv4.3 as bait in a yeast two-hybrid screen of a rat midbrain cDNA library and identified two members of a calcium-binding protein family, KChIPs (Kv channel interacting proteins) 1 and 2, that are highly expressed in the CNS and interact with Kv4 but not other Kv α subunits (An et al., 2000). Coexpression of KChIP1, KChIP2, or a third family member, KChIP3, dramatically increases density, slows inactivation kinetics, and speeds the rate of recovery from inactivation of Kv4 channels expressed in heterologous cells (An et al., 2000; Bahring et al., 2001; Holmqvist et al., 2002; Shibata et al., 2003; Patel et al., 2004). KChIP4 can have distinct effects, depending on a splice variant-specific unique N terminus (Holmqvist et al., 2002; Shibata et al., 2003). Kv4 α subunits and KChIPs form

Received March 4, 2004; revised July 29, 2004; accepted July 29, 2004.

This work was supported by Wyeth Research and by National Institutes of Health Grant NS42225 (J.S.T.). We thank Dr. Pranab Chanda and Wade Edris for preparation and purification of KChIP fusion proteins, Dr. Gail Mandel for the use of the confocal microscope and luminometer, and Drs. Mark Bowlby, John Moyer, James Barrett, Peter DiStefano, and Kevin Willis for support and encouragement during the course of this work.

Correspondence should be addressed to Dr. James S. Trimmer, Department of Pharmacology, 1311 Tupper Hall, School of Medicine, University of California, One Shields Avenue, Davis, CA 95616-8635. E-mail: jtrimmer@ucdavis.edu.

K. J. Rhodes's present address: Neurological Disorders, Johnson and Johnson Pharmaceutical Research and Development, Raritan, NJ 08869.

DOI:10.1523/JNEUROSCI.0776-04.2004

 0270-6474/04/247903-13$15.00/0

$Kv4_4KChIP_4$ octomeric complexes (Kim et al., 2004a), with the KChIPs interacting with the Kv4 N termini (Scannevin et al., 2004; Zhou et al., 2004) in a large cytoplasmic structure in which the KChIPs appear to enwrap the "hanging gondola" formed by the Kv4 N termini (Kim et al., 2004b).

Here, we describe in detail the distribution, colocalization, and coassociation of Kv4.2, Kv4.3, and KChIPs 1, 2, 3 (An et al., 2000), and 4 (Holmqvist et al., 2002) in adult rat brain. We generated and characterized monoclonal antibodies (mAbs) specific for each Kv4 or KChIP polypeptide and used these reagents for immunohistochemical and multiple-label immunofluorescence and coimmunoprecipitation analyses to map the loci of KChIP/Kv4 interaction. We also used circumscribed ibotenic acid lesions within the hippocampal formation and immunohistochemistry (Monaghan et al., 2001) to confirm the somatodendritic localization of KChIP and Kv4 immunoreactivity.

Table 1. Sequences of peptide and fusion protein antigens used to generate Kv4- and KChIP-specific antibodies

Subunit	Antigen (aa residues)	Sequence	Hybridoma	Sequence reference
Kv4.2-E	209–225	CGSSPGHIKELPSGERY	K57/27.1	Baldwin et al., 1991
Kv4.3-C	GST-415–636	C-terminal tail	K75/30.1	Tsaur et al., 1997
KChIP1	GST-KChIP1	Full-length GST fusion	K55/7.1	An et al., 2000
Pan-KChIP	GST-KChIP1	Full-length GST fusion	K55/82.1*	An et al., 2000
KChIP2	GST-KChIP2	Full-length GST fusion	K60/73.1	An et al., 2000
KChIP3	GST-KChIP3	Full-length GST fusion	K66/36.1	An et al., 2000
KChIP4	GST-KChIP4	Full-length GST fusion	1G2	Holmqvist et al., 2002

C denotes cysteine residue added for conjugation to KLH or BSA. *This antibody recognizes all KChIP family members.

Materials and Methods

Materials. Reagents were molecular biology grade from Sigma (St. Louis, MO) or Roche Diagnostics (Indianapolis, IN), except where noted otherwise. Alexa-488 and Alexa-594 fluorophore-conjugated isotype-specific antibodies were purchased from Molecular Probes (Eugene, OR). Biotin-conjugated anti-mouse isotype-specific antibodies were purchased from Southern Biotechnology (Atlanta, GA). Precast, neutral pH (NuPAGE) gels were used for all SDS-PAGE experiments and were purchased from Invitrogen (Carlsbad, CA).

Generation and characterization of KChIP and Kv4 antibodies. Mouse monoclonal and affinity-purified rabbit polyclonal antibodies were generated and purified essentially as described previously (Trimmer, 1991; Rhodes et al., 1995, 1996; Bekele-Arcuri et al., 1996). Peptide or fusion protein sequences used to generate antibodies against Kv4.2, Kv4.3, KChIP1, KChIP2, KChIP3, or KChIP4 are listed in Table 1. Rabbits were immunized with purified recombinant glutathione *S*-transferase (GST) fusion proteins or with synthetic peptides [Quality Controlled Biochemicals (Hopkinton, MA) or Research Genetics (Huntsville, AL)] conjugated to keyhole limpet hemocyanin. Antibody titers were determined by ELISA against the cognate synthetic peptide or fusion protein immunogen. In cases in which GST fusion proteins were used as the immunogen, titers against the GST fusion protein were compared with titers against GST protein alone. Rabbit polyclonal antibodies were affinity purified on immobilized peptide or fusion protein affinity columns using standard procedures (Rhodes et al., 1995).

BALB/c mice used for the production of mAbs were obtained from Taconic Farms (Germantown, NY). The myeloma cell line SP2/0 was generously provided by Dr. I. S. Trowbridge (The Salk Institute, La Jolla, CA). BALB/c mice were first immunized with an intraperitoneal injection containing 100 μg of Kv4 or KChIP immunogen resuspended in 50% RIBI adjuvant system MPL+TDM emulsion R-700 (RIBI Immunochem, Hamilton, MT) in phosphate-buffered saline (PBS; 150 mM NaCl and 10 mM sodium phosphate, pH 7.4). Mice were subsequently immunized with 50 μg of immunogen on days 14 and 21. Sera were collected on days 10, 17, and 21 and screened for immunoreactivity against the Kv4 or KChIP immunogen by ELISA using a goat anti-mouse IgG-specific secondary antibody. The mouse that displayed the more mature immune response received 50 μg of immunogen in PBS intravenously on days 28–30 and was killed for splenectomy on day 31.

Hybridomas were produced by standard methodology (Trimmer et al., 1985; Bekele-Arcuri et al., 1996). In brief, spleen cells were dissociated and fused with polyethylene glycol to SP2/0 mouse myeloma cells at a ratio of 10:1 spleen cells to myeloma cells, and the resultant fusion mixture was plated into 10 96-well tissue culture plates. Hybridomas were selected for growth in media containing hypoxanthine, aminopterin, and thymidine for 14 d; media containing hypoxanthine and thymidine were used for the third week. Ten to 14 d after the fusion, tissue culture supernatants were screened by ELISA against COS-1 cells transiently transfected with cDNAs encoding the appropriate full-length Kv4 or KChIP polypeptide. Bound mAb was detected by luminometry. In each case, large pools of positive clones were obtained for additional analysis (K57:48; K75:48; K55:96; K60:36; K66:60). Samples exhibiting positive reactions were expanded, and the resulting culture supernatants were screened by immunofluorescence staining of COS-1 cells transiently transfected with cDNAs encoding the appropriate full-length Kv4 or KChIP polypeptide. The same sample set was also screened for specific immunoreactivity on immunoblots of rat brain membranes and for immunoperoxidase staining of rat brain sections. Specificity for distinct Kv4 or KChIP isoforms was verified by immunofluorescence staining and immunoblot analyses of COS-1 cells transiently transfected with cDNAs encoding the entire set of full-length Kv4 or KChIP polypeptides, by competition experiments to show elimination of staining of brain sections by preincubation with the appropriate peptide/fusion protein immunogen, and by verification that cellular immunocytochemical staining patterns matched gene expression patterns obtained from *in situ* hybridization analyses. Selected hybridomas were then subcloned by limiting dilution, reassayed, and grown in BALB/c mice for production of ascites fluid as described previously (Trimmer et al., 1985). Immunoglobulins were purified by ammonium sulfate precipitation, followed by DEAE chromatography, as described (Trimmer et al., 1985).

Immunoprecipitation. Immunoprecipitation reactions were performed at 4°C using detergent lysates of crude membranes (Trimmer, 1991) isolated from freshly dissected adult rat brain. In brief, membranes derived from whole brain or individual brain regions as indicated (0.5 mg of membrane protein/tube) were solubilized in radioimmunoprecipitation assay (RIPA) buffer [1% IGEPAL CA-630, 0.5% deoxycholic acid, 0.1% SDS, 0.15 M NaCl, and 50 mM Tris-HCl, pH 7.4, containing protease inhibitor mixture (Roche Diagnostics)]. Affinity-purified rabbit polyclonal or mouse mAbs specific for each antigen were added, and the volume was adjusted with RIPA buffer to 0.1 ml per reaction tube. Sixty microliters of 50% slurry of protein A agarose (Pierce, Rockford, IL) were added to each tube, and the samples were incubated at 4°C overnight on a rocker table. After incubation, protein A agarose was centrifuged at 14,000 × *g* for 20 sec, and the resulting pellets were washed by resuspension and centrifugation four times with lysis buffer (1% Triton X-100, 0.15 M NaCl, 1 mM EDTA, 10 mM sodium azide, and 10 mM Tris-HCl, pH 8.0). The final pellets were resuspended in 80 μl of 2× reducing sample buffer.

SDS-polyacrylamide gels and immunoblotting. Pellets from immunoprecipitation reactions were heated to 50°C for 10 min, vortexed, and centrifuged to pellet the agarose. Thirty microliters of each sample were size fractionated on 4–12% gradient (for analysis of Kv4 α subunits) or 10% (for analysis for KChIP proteins) precast NuPAGE gels. After electrophoretic transfer to nitrocellulose membrane, the resulting blots were blocked in Tris-buffered saline (20 mM Tris, pH 7.6, and 0.137 M NaCl) containing 5% nonfat dried milk and 0.1% Tween 20. The blots were incubated in purified antibody diluted in the blocking agent overnight at 4°C, washed three times for 10 min in TBS–Tween, and then incubated for 1 hr at room temperature in a blocking agent containing HRP-conjugated secondary antibody (Jackson ImmunoResearch, West Grove, PA). After another three 10 min washes in TBS–Tween, the membranes were incubated in substrate for enhanced chemiluminescence (ECL; Am-

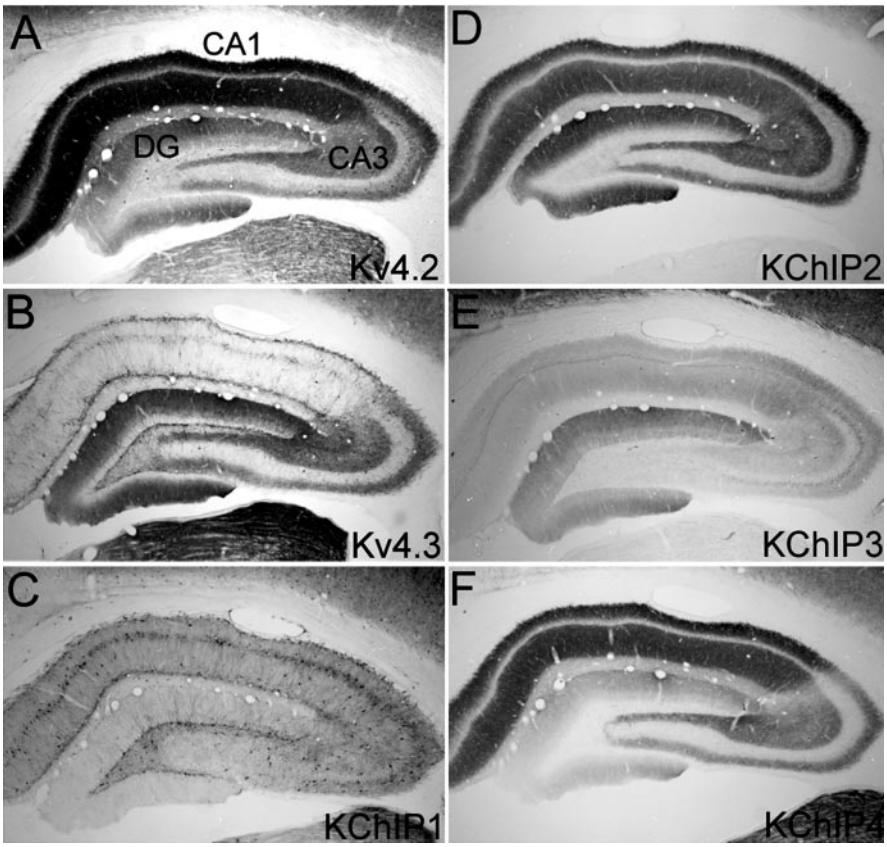

Figure 1. Immunohistochemical localization of Kv4 α subunits and KChIPs in the hippocampal formation. Photomicrographs of coronal sections taken to show the areal and laminar distribution of Kv4.2 (*A*), Kv4.3 (*B*), KChIP1 (*C*), KChIP2 (*D*), KChIP3 (*E*), and KChIP4 (*F*) immunoreactivity in the rat hippocampus are shown. Immunoreactivity for Kv4.2, KChIP2, KChIP3, or KChIP4 is concentrated in dendritic fields, including the apical dendritic fields of dentate granule cells and the apical and basal dendrites of CA and subicular pyramidal cells. In the dentate gyrus and CA3 subfields, immunoreactivity for Kv4.3 is concentrated in granule and pyramidal cell dendrites. However, in these subfields, Kv4.3 immunoreactivity is also concentrated in the somata and dendrites of large multipolar interneurons. In all hippocampal subfields, immunoreactivity for KChIP1 is concentrated in the cell bodies and throughout the dendritic trees of large multipolar interneurons. DG, Dentate gyrus.

ersham, Arlington Heights, IL) for 1 min. The excess ECL substrate was removed and the blots exposed to Hyperfilm-ECL film (Amersham).

Experimental localization of channel subunits. All surgical procedures were approved by the Wyeth Institutional Animal Care and Use Committee and were in accordance with the *NIH Guide for the Care and Use of Laboratory Animals*. Before surgery, animals were anesthetized deeply with sodium pentobarbital (50 mg/kg, i.p.) and secured in a stereotaxic carrier (David Kopf Instruments, Tajunga, CA). Ibotenic acid lesions of hippocampal subfields were performed as described previously (Monaghan et al., 2001). In brief, ibotenic acid (0.1–0.4 μl of a 10 μg/μl solution in 0.1 M sodium phosphate buffer, pH 7.4) was injected directly into the target structure using a 2 μl Hamilton microsyringe mounted in a Kopf microsyringe microdrive. In some of these animals, injections were made at two or three depths, with each injection separated in the dorsoventral axis by 2.5 mm.

Immunohistochemistry. Animals that sustained surgery were killed 7 d postoperatively. At the time of death, all animals were anesthetized deeply with sodium pentobarbital (60 mg/kg, i.p.) and then perfused through the ascending aorta with 0.1 M $NaPO_4$ buffer, pH 7.4, followed by fixative containing freshly depolymerized 4% paraformaldehyde in 0.1 M $NaPO_4$ buffer. The remaining procedures for light microscopic immunohistochemistry were described in detail previously (Rhodes et al., 1995, 1996). All of the immunohistochemical and immunofluorescence data presented here were collected on sections processed using the purified mouse mAbs described in Results, with the exception of staining for Kv2.1, which used an affinity-purified rabbit polyclonal antibody ("KC") described previously (Trimmer, 1991; Rhodes et al., 1995, 1996; Monaghan et al., 2001). Briefly, 40-μm-thick horizontal sections were incubated overnight at 4°C in antibody vehicle containing purified mouse mAb. Detection of antibody–antigen complexes was accomplished using the ABC *Elite* peroxidase reaction kit (Vector Laboratories, Burlingame, CA) and visualized using a nickel-enhanced diaminobenzidine procedure (Tago et al., 1986; Rhodes et al., 1995). Double-label immunofluorescence labeling was performed as described previously (Rhodes et al., 1997), except that isotype-specific anti-mouse antibodies conjugated to Alexa fluorophores (Molecular Probes) were used as the detecting antibodies.

Diaminobenzidine-stained and immunofluorescence sections were analyzed and imaged using an Axiophot photomicroscope and confocal microscope (Zeiss, Thornwood, NY) equipped with argon lasers. Black-and-white 35 mm film negatives containing photomicrographs of stained sections were digitized using a Nikon LS1000 35 mm film scanner. The scanned and/or digital images were arranged and labeled in Adobe Photoshop with only minor adjustments of image brightness and contrast.

Results

Characterization of anti-KChIP and anti Kv4 mAbs

The KChIP polypeptides have variable N termini but share 70% identity throughout their C-terminal 185 amino acids (An et al., 2000; Holmqvist et al., 2002). Initially, we focused our efforts to generate KChIP-specific antibodies on the variable N termini. Although we were successful in obtaining high-titer rabbit polyclonal antibodies using this approach, whereas these antibodies were specific for the target protein, these antibodies did not yield crisp immunohistochemical staining of brain sections. In a second attempt to generate high-quality reagents for immunohistochemistry, we generated GST fusion proteins encoding each full-length KChIP polypeptide and used these as immunogens to generate mouse mAbs. To identify anti-KChIP mAbs that reacted specifically with the desired KChIP polypeptide and not other antigens, hybridoma supernatants from the KChIP immunizations were screened by ELISA versus the cognate immunogen, by immunofluorescence staining versus a panel of transiently transfected COS cells expressing the entire set of full-length Kv4 or KChIP polypeptides (data not shown), and subsequently by immunoblotting versus cell lysates prepared from transiently transfected COS cells (supplemental material, available at www.jneurosci.org). Using this strategy, from large pools of positive mAbs (see Materials and Methods for details) we identified and subsequently purified mAbs that specifically recognized the cognate Kv4 or KChIP antigen and not other proteins.

A representative assay of specificity is shown in the supplemental material (available at www.jneurosci.org). By immunoblotting samples from transfected mammalian cells, each of the selected mAbs recognized a major band corresponding to the appropriate Kv4 or KChIP polypeptide and did not cross-react with other highly related family members. In the immunoblots

probed with antibodies against Kv4.2 or Kv4.3, we always observed immunoreactivity with high molecular weight bands. These bands represent dimers and larger aggregates of Kv4.2 or Kv4.3 (supplemental material, available at www.jneurosci.org) (Sheng et al., 1993; An et al., 2000). We confirmed that these higher molecular weight bands are aggregated Kv4 α subunits by stripping and reprobing the immunoblots with anti-Kv4 antibodies directed at epitopes elsewhere in the Kv4 sequence. These disparate anti-Kv4 antibodies recognized these same high molecular weight bands identified by the anti-Kv4 mAbs (data not shown), confirming that the high molecular weight aggregates contain Kv4 α subunits. In the immunoblots probed with anti-KChIP3 mAbs, we always observed immunoreactivity with a lower molecular weight (~20 kDa) band (supplemental material, available at www.jneurosci.org). Presumably, this band represents a KChIP3 N-terminal cleavage product, as reported previously (Tekirian et al., 2001). This lower molecular weight band is observed only in lysates prepared from COS cells transfected with KChIP3, making it is highly unlikely that this second band indicates cross-reactivity of the anti-KChIP3 mAb with another protein.

To further verify the specificity of the anti-KChIP antibody reagents used for immunohistochemistry, competition experiments were performed in which each anti-KChIP antibody was incubated with either the cognate recombinant KChIP protein antigen or with one of the other recombinant KChIP polypeptides. We observed that immunohistochemical staining was completely inhibited by incubation with the cognate KChIP antigen but not with recombinant proteins encoding other KChIP family members (data not shown). We also verified that cellular immunocytochemical staining patterns matched gene expression patterns obtained from *in situ* hybridization analyses. It is also important to note that in our screen of anti-KChIP hybridomas we identified several hybridomas that secreted mAbs recognizing more than one, or even all, KChIP polypeptides (so-called "pan-KChIP" antibodies) (Table 1) (An et al., 2000). Table 1 lists the mAbs that were used for the immunohistochemical analyses described below.

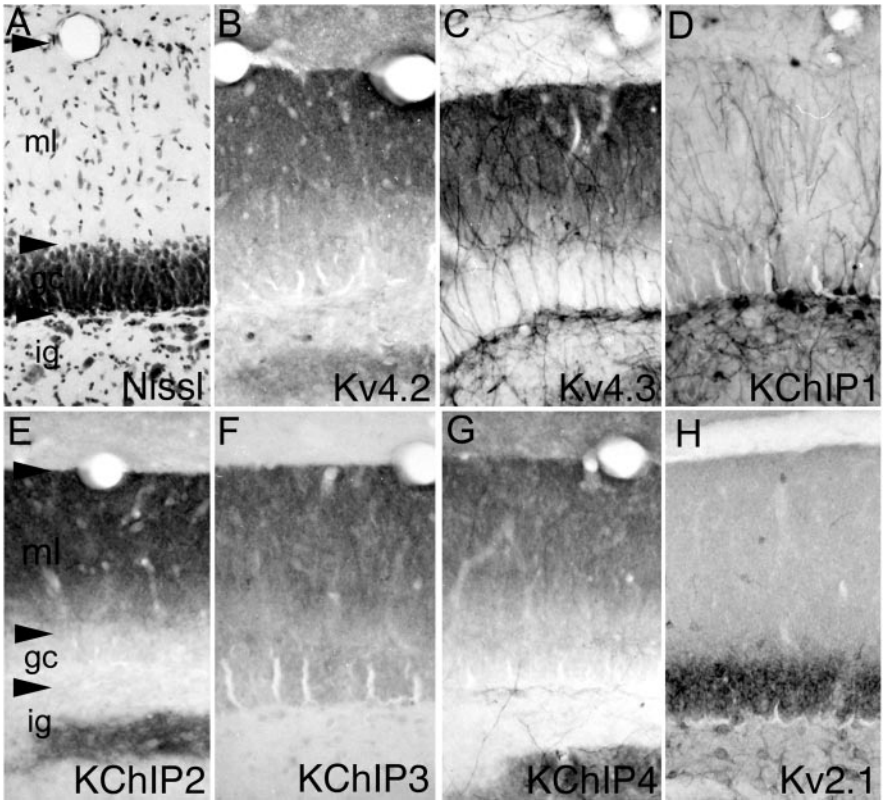

Figure 2. Distribution of Kv4 α subunits and KChIPs in the dentate gyrus. In the dentate gyrus (cellular architecture shown by the Nissl stain in *A*), a high density of immunoreactivity for Kv4.2 (*B*), Kv4.3 (*C*), and KChIPs 2–4 (*E–G*, respectively) is concentrated throughout the molecular layer, where the staining appears to be concentrated in the dendrites of dentate granule cells. This extensive dendritic staining contrasts with the distribution of immunoreactivity for Kv2.1 (*H*), which is confined to the soma and proximal dendrites only. There is also a moderate to high density of immunoreactivity for Kv4.2, Kv4.3, and KChIPs 2–4 in the infragranular zone, where the staining is concentrated in the dendritic fields of hilar neurons. In the infragranular zone, immunoreactivity for Kv4.3 and KChIP1 is concentrated in the somata and dendrites of large interneurons, presumably dentate mossy cells, the dendrites of which extend across the entire width of the molecular layer. ig, Infragranular layer; gc, granule cell layer; ml, molecular layer.

Immunohistochemistry

Because a comprehensive description of the patterns of KChIP and Kv4 α subunit immunoreactivity is well beyond the scope or intent of this report, we focused our analyses and descriptions on brain regions and cell types in which somatodendritic A-currents have been the most intensely studied: the hippocampal formation, neocortex, and striatum. We reasoned that the wealth of published electrophysiological data would allow us to draw reasonable inferences about the relationships between the Kv4 and KChIP staining patterns and the underlying currents in these brain regions.

As described in more detail below, immunoreactivity for Kv4 α subunits and KChIPs is concentrated primarily in the dendrites and somata of central neurons. The staining associated with labeled dendrites tends to be quite uniform, with little evidence of local concentrations of immunoreactivity at synapses or on dendritic spines. For comparison and contrast with the pattern of Kv4 and KChIP immunoreactivity, in most of the figures we show immunohistochemical staining for Kv2.1, a delayed rectifier Kv channel expressed in the somata and proximal dendrites of rat central neurons (Trimmer, 1991; Rhodes et al., 1995, 1996; Scannevin et al., 1996; Du et al., 1998).

The hippocampal formation

The staining pattern for Kv4.2, Kv4.3, and all four KChIP polypeptides across hippocampal subfields and laminas is shown in Figure 1. Higher magnification micrographs of the staining patterns within individual hippocampal subfields are shown in Figures 3–5. Overall, there is a high density of immunoreactivity and a close correspondence in the staining patterns for Kv4.2, Kv4.3, and KChIPs 2, 3, and 4 in the dentate gyrus and CA subfields. There is also a close correspondence between the staining patterns for Kv4.3 and KChIP1, particularly in the dentate hilus and CA1 subfields, where immunoreactivity for these two Kv channel subunits is concentrated in the somata and dendrites of large multipolar interneurons.

In the dentate gyrus, immunoreactivity for Kv4.2, Kv4.3, and

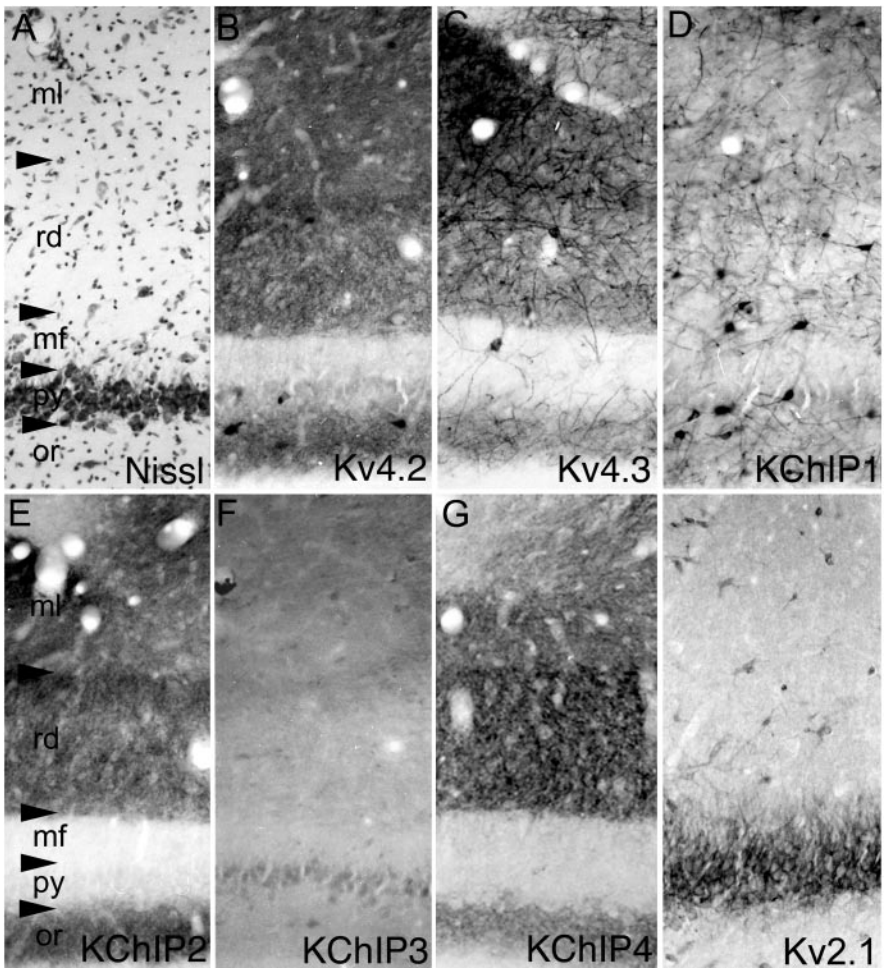

Figure 3. Distribution of Kv4 and KChIP immunoreactivity in the CA3 subfield. In the CA3 subfield (cellular architecture shown by the Nissl stain in *A*), immunoreactivity for Kv4.2 (*B*), Kv4.3 (*C*), KChIP2 (*E*), and KChIP4 (*G*) is concentrated in the apical and basal dendrites and fine dendritic branches of pyramidal cells. There is little, if any, observable immunoreactivity for these subunits in the somata of CA3 pyramidal cells. Although there is also immunoreactivity for KChIP3 (*F*) in CA3 pyramidal cell dendrites, the density of KChIP3 immunoreactivity is far lower than KChIPs 2 or 4. Interestingly, there is a greater density of Kv4 and KChIP immunoreactivity in the proximal two-thirds of the dendritic fields of CA3 pyramidal cells (stratum radiatum) than in the distal third (stratum moleculare). These staining patterns contrast sharply with that for Kv2.1 (*H*), which is restricted to the proximal one-third of the larger-caliber apical and basal dendritic branches. As in the dentate gyrus, immunoreactivity for Kv4.3 and KChIP1 (*D*) is concentrated in the somata and dendrites of large, multipolar interneurons. These Kv4.3- and KChIP1-immunoreactive interneurons are concentrated in the stratum oriens (or), stratum pyramidale (py), and stratum radiatum (rd); few KChIP1- or Kv4.3-positive interneurons are observed in the stratum lacunosum moleculare (ml). mf, Stratum lucidum.

KChIPs 2, 3, and 4 is concentrated throughout in the molecular layer, where the staining appears to be associated with the dendrites of dentate granule cells (Fig. 2). Surprisingly, there is little or no staining for these subunits in the perinuclear cytoplasm of dentate granule cells despite the high levels of expression of Kv4.2, Kv4.3, KChIP2, KChIP3, and KChIP4 mRNA in dentate granule cell somata (Serôdio and Rudy, 1998, their Fig. 3; M. M. Monaghan, B. W. Strassle, M. A. Sung, W. F. An, and K. J. Rhodes, unpublished observations). Across the molecular layer of the dentate gyrus, the density of Kv4 and KChIP immunoreactivity is not uniform; there is a greater density of immunoreactivity in the outer two-thirds of the molecular layer compared with the inner third (Fig. 2 and supplemental material, available at www.jneurosci.org). This staining pattern suggests that there is a greater density of Kv4-mediated A-type currents in distal dendrites of dentate granule cells compared with the more proximal dendrites. Immunoreactivity for KChIP1, together with Kv4.3, is concentrated in the somata and dendrites of large multipolar interneurons located within the infragranular zone and granule cell layer of the dentate gyrus. The dendrites of these large interneurons are very intensely labeled, and there is also a high density of immunoreactivity for Kv4.3 and KChIP1 in the perinuclear cytoplasm of these cells.

In the CA3 subfield, there is a moderate to high density of immunoreactivity for Kv4.2, Kv4.3, KChIP2, and KChIP4 and a low density of immunoreactivity for KChIP3 (Fig. 3). The immunoreactivity for these subunits is concentrated in the stratum oriens and stratum radiatum, where the staining appears to be associated with the apical and basal dendrites of CA3 pyramidal cells. There is little or no staining for these subunits within the stratum lucidum (mossy fiber zone) or, surprisingly, in the stratum moleculare. As in the dentate gyrus, there is very little, if any, Kv4 or KChIP immunoreactivity within the perinuclear cytoplasm of CA3 pyramidal cells. In CA3, immunoreactivity for KChIP1 and Kv4.3 is concentrated in the somata and dendrites of large multipolar interneurons. These interneurons have thick dendrites that are very intensely labeled for Kv4.3 and KChIP1.

In the CA2 and CA1 subfields, immunoreactivity for Kv4.2, KChIP2, KChIP3, and KChIP4 is concentrated in the stratum oriens and stratum radiatum and appears to be associated with the apical and basal dendritic arbors of pyramidal cells (Fig. 4). As described for CA3, there is little staining in the perinuclear cytoplasm of CA1 or CA2 pyramidal cells. Interestingly, as in CA3, at the junction of the stratum radiatum and stratum moleculare, there is a very abrupt decrease in the intensity of immunoreactivity for Kv4.2, KChIP2, KChIP3, and KChIP4, suggesting that there is a far lower density of Kv4 channels, and presumably A-type currents, in the far distal and apical dendritic tufts of CA1 (and CA3) pyramidal cells compared the apical and basal dendrites in the stratum radiatum and oriens or the fine dendritic branches contained within the stratum radiatum. A subtle gradient in Kv4.2 expression is also observed in the stratum radiatum of CA1 (Fig. 2 and supplemental material, available at www.jneurosci.org).

In stark contrast to CA3, in the CA1 subfield, immunoreactivity for Kv4.3 is concentrated exclusively in large multipolar interneurons; there is little, if any, detectable Kv4.3 staining in the apical or basal dendrites of CA1 pyramidal cells. The cellular patterns of staining for Kv4.2 and Kv4.3 protein in the CA subfields match well to that predicted from previous *in situ* hybridization studies (Serôdio and Rudy, 1998). This dramatic difference in the distribution of Kv4.3 protein between CA3 and CA1 suggests that there is a shift in the α subunit composition of Kv4 channels in CA3 pyramidal cell dendrites versus those in CA1,

with likely heteromeric channels containing Kv4.2 and Kv4.3 in CA3 pyramidal cell dendrites but predominantly homomeric channels containing Kv4.2 α subunits without coassociated Kv4.3 in CA1 pyramidal cell dendrites. In CA1, as elsewhere in the hippocampus, immunoreactivity for KChIP1 is confined to large multipolar interneurons, and there is a very close correspondence between the patterns of KChIP1 and Kv4.3 immunoreactivity in these cells.

To confirm that the staining patterns for Kv4 and KChIP polypeptides in the hippocampal formation reflected localization of these subunits to cell bodies and dendrites and not to axons and terminal fields, we made circumscribed ibotenic acid lesions within individual hippocampal subfields and then examined the effects of these lesions on the distribution and density of immunoreactivity for each subunit. We previously confirmed that this lesion strategy destroys neurons but spares axons and terminals within the boundaries of the lesion, and we also described in detail the technical details and caveats to the interpretation of data obtained from this strategy (Monaghan et al., 2001).

Ten rats sustained unilateral injections of the neurotoxin ibotenic acid into the hippocampal formation. Each injection was targeted to either the dentate gyrus or the CA1 subfield. Although the injections generally destroyed neurons within the targeted subfield, there was variable spread of the neurotoxin into adjacent subfields. An example of an ibotenic acid lesion into the distal CA1 subfield is shown in Figure 5. This lesion destroyed neurons within the distal half of the CA1 subfield, the prosubiculum, and subiculum, and also spread across the hippocampal fissure to destroy neurons within the central portion of the dentate gyrus. The loss of neuronal somata and dendrites was confirmed by the loss of immunoreactivity for Kv2.1 within the boundaries of the lesion (outlined in Fig. 5*H*). As expected, there was a dramatic decrease in the density of immunoreactivity for Kv4.2, Kv4.3, and all four KChIP polypeptides within and precisely at the boundaries of the ibotenic acid lesion, and there was no change in the distribution or density of immunoreactivity within subfields that receive afferent input from the affected area. These data confirm that within the dentate gyrus, CA1 subfield, and subiculum, these subunits are localized to neuronal somata and dendrites as opposed to afferent axons and terminals. Ibotenic acid lesions that destroyed neurons within the CA3 subfield also produced a loss of Kv4 and KChIP immunoreactivity within the boundaries of the lesion (data not shown), indicating that in all hippocampal subfields, Kv4 α subunits and KChIPs are located postsynaptically on the somata and dendrites of hippocampal neurons. This localization of Kv4 α subunits and KChIPs stands in sharp contrast to the location of Kv1 channels on afferents and nerve terminals, as determined using the same ibotenic acid lesion strategy (Monaghan et al., 2001).

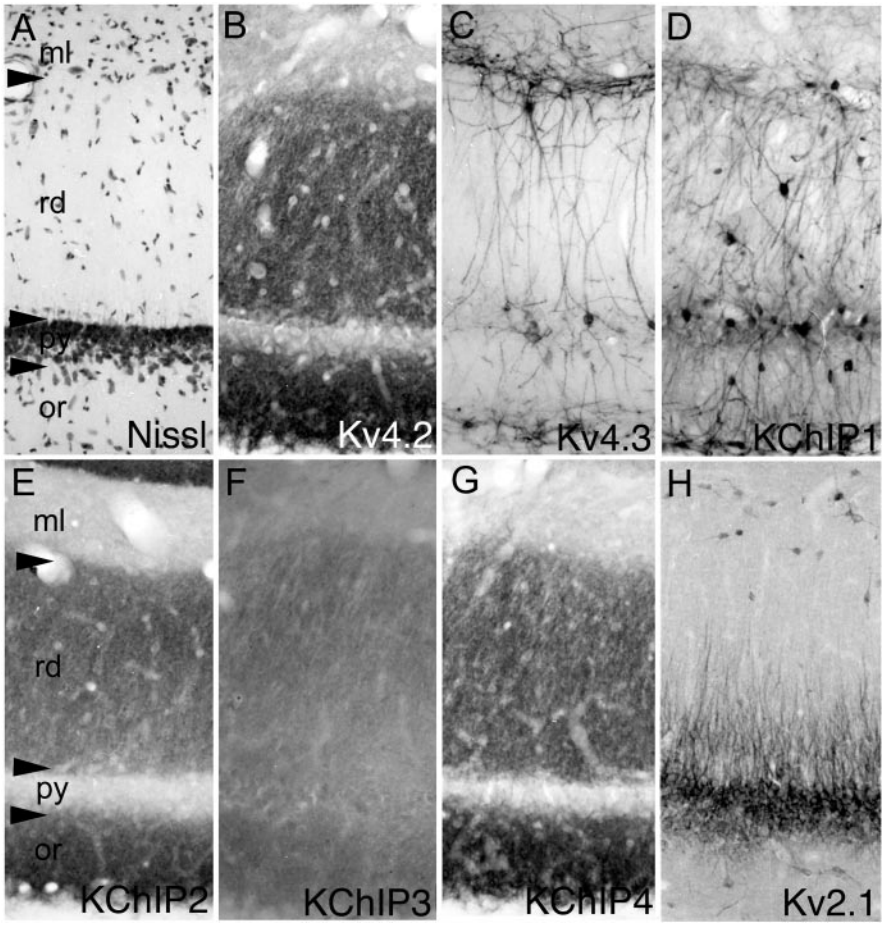

Figure 4. Distribution of Kv4 and KChIP immunoreactivity in the CA1 subfield. In the CA1 subfield (cellular architecture shown by the Nissl stain in *A*), immunoreactivity for Kv4.2 (*B*), KChIP2 (*E*), and KChIP4 (*G*) but not Kv4.3 (*C*) is concentrated in the apical and basal dendrites and fine dendritic branches of pyramidal cells. There is little, if any, observable immunoreactivity for these subunits in the somata of CA1 pyramidal cells. Although there is also immunoreactivity for KChIP3 (*F*) in CA1 pyramidal cell dendrites, the density of KChIP3 immunoreactivity is far lower than KChIPs 2 or 4. As in CA3, there is a far greater density of Kv4.2, KChIP2, and KChIP4 immunoreactivity in the proximal two-thirds of the dendritic fields of CA3 pyramidal cells (stratum radiatum) compared with the distal third (stratum moleculare). These staining patterns contrast sharply with that for Kv2.1 (*H*), which is strikingly restricted to the proximal one-third of the larger-caliber apical and basal dendritic branches. As in the dentate gyrus and CA3 subfields, immunoreactivity for Kv4.3 and KChIP1 (*D*) is concentrated in the somata and dendrites of large, multipolar interneurons. These Kv4.3- and KChIP1-immunoreactive interneurons are concentrated in the stratum oriens (or), stratum pyramidale (py), stratum radiatum (rd), and along the junction of stratum radiatum and stratum moleculare. Interestingly, it appears that total number of Kv4.3-positive interneurons is a subset of those that are immunoreactive for KChIP1. ml, Stratum lacunosum moleculare.

Posterior cingulate cortex

Previous descriptions of the pattern of Kv4.3 mRNA and protein expression in brain noted the very high levels Kv4.3 expression and immunoreactivity in the posterior cingulate cortex (Area 23) (Tsaur et al., 1997). To confirm and extend these observations, we examined the distribution of immunoreactivity for Kv4 α subunits and KChIPs in this brain region. As shown in Figure 6, there is an exceptionally high density of immunoreactivity for Kv4.3 in the somata and dendrites of large neurons in layer II of the posterior cingulate cortex. Staining in these cells is concentrated in the apical dendrites that extend in bundles into layer I. Although there is a far lower density of immunoreactivity for Kv4.2 compared with Kv4.3 in these cells, the high density of Kv4.3 immunoreactivity is matched by a similarly high density of

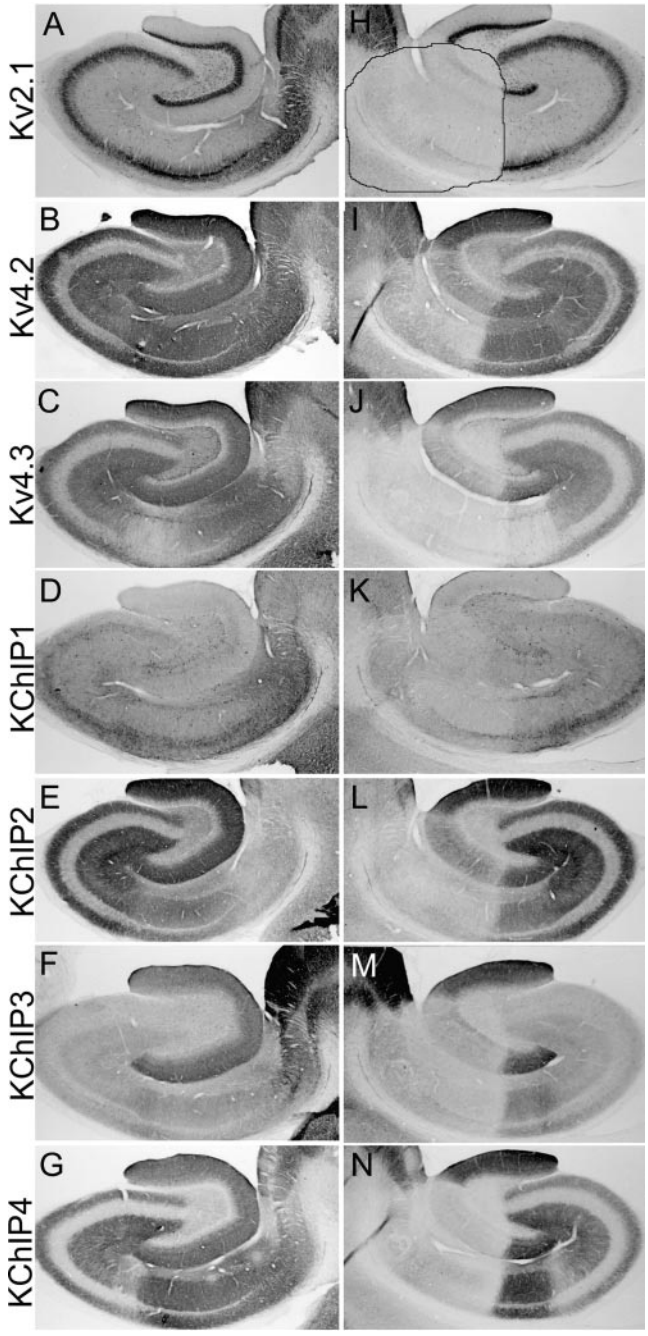

Figure 5. Effects of an ibotenic acid lesion on the distribution and density of Kv4 and KChIP immunoreactivity in the hippocampal formation. These photomicrographs show the pattern of immunoreactivity for the indicated subunits in the unoperated, control hemisphere (*A–G*) and operated hemisphere (*H–N*) of an animal that sustained a circumscribed unilateral ibotenic acid lesion. This lesion destroyed cells in the distal CA1 subfield, prosubiculum, and subiculum and also destroyed a central portion of the dentate gyrus. The entire CA3 and proximal CA1 subfield was spared by this lesion. The pattern of cell loss is clearly indicated by the loss of Kv2.1 immunoreactivity within the boundaries of the lesion (outlined in *H*). This lesion greatly reduced the density of Kv4.2 (compare *B*, *I*), Kv4.3 (compare *C*, *J*), and KChIP1–4 (compare *D–G*, *K–N*) immunoreactivity within the boundaries of the lesion, indicating that these subunits are localized to the cell bodies and/or dendrites of dentate granule cells and CA1 pyramidal cells or, in the case of Kv4.3 and KChIP1, to the cell bodies and dendrites of dentate and CA1 interneurons.

KChIP4 staining. In addition, there is a moderate density of KChIP2 in the somata and dendrites of the layer II neurons and the pattern of staining matches that observed for Kv4.3, Kv4.2, and KChIP4. In the deeper cortical layers of the posterior cingulate cortex, there is a moderate density of immunoreactivity for Kv4.2, KChIP2, and KChIP4 in the somata and apical dendrites of pyramidal cells located in layers V and VI. The staining in the apical dendrites of these cells is readily apparent as fascicles of dendrites ascending through the more superficial cortical laminas to enter layer I. In the cingulate cortex as in the hippocampal formation, immunoreactivity for Kv4.3 and KChIP1 is concentrated within small and large bipolar and multipolar interneurons scattered throughout layers II–VI. These cells are very intensely stained for KChIP1, where immunoreactivity is concentrated in the somata as well as the dendritic arbors.

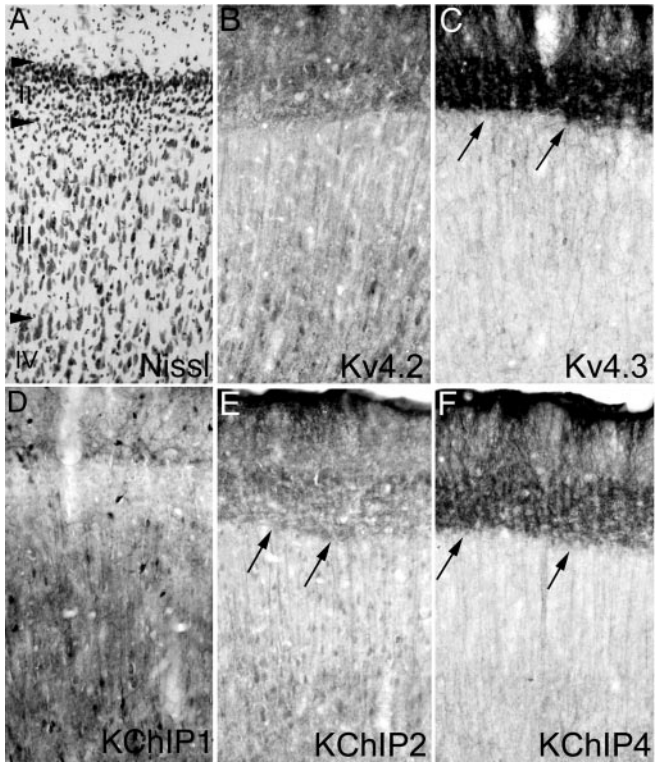

Figure 6. Distribution of Kv4 and KChIP immunoreactivity in the posterior cingulate cortex. In the posterior cingulate cortex (cellular architecture shown by the Nissl stain in *A*), there is a very high density of immunoreactivity for Kv4.3 (*C*) and KChIP4 (*F*) in the somata and dendrites of neurons in layer II. These neurons have thick dendrites that extend in bundles up into layer I. These cells also have a low to moderate density of immunoreactivity for Kv4.2 (*B*) and KChIP2 (*E*). In the deeper cortical layers, there is a moderate density of immunoreactivity for Kv4.2 and KChIPs 2 and 4. This immunoreactivity is concentrated in pyramidal cells and can be observed in fascicles of apical dendrites ascending through the more superficial cortical layers. Immunoreactivity for KChIP1 (*D*) and Kv4.3 is concentrated in bipolar and multipolar interneurons scattered throughout layers II–VI of the posterior cingulate cortex.

Neocortex

The pattern of immunoreactivity for Kv4.2, Kv4.3, KChIPs 1–4, and Kv2.1 in the parietal sensorimotor cortex is shown in Figure 7. As in the posterior cingulate cortex, immunoreactivity for Kv4.2 is concentrated in the somata and apical dendrites of cortical pyramidal cells. There is a very high density of immunoreactivity for Kv4.2 in pyramidal cells in layers II and III, and there is also a high density of immunoreactivity for Kv4.2 in layer V pyramidal cells, where the staining can be followed along the entire apical dendrite and extending into apical dendritic tufts in layer I. Although this pattern of immunoreactivity for Kv4.2 is matched by a similar pattern of immunoreactivity for KChIPs 2,

3, and 4, it is clear that the pattern of KChIP3 and KChIP4 immunoreactivity most closely matches the staining pattern for Kv4.2. For KChIP2, there is a much greater density of immunoreactivity in the apical dendrites of layer II–III pyramidal cells compared with the density of staining in layer V neurons, and there is also a very high density of immunoreactivity for KChIP2 in layer IV, where the staining is concentrated in small multipolar neurons and perhaps also in afferent fibers. The immunoreactivity for Kv4.2 and KChIPs 2, 3, and 4 in fascicles of apical dendrites of cortical pyramidal cells stands out in marked contrast to the staining for Kv2.1. Kv2.1 immunoreactivity is restricted to the proximal portion of the apical and basal dendrites, whereas the immunostaining for Kv4.2 and these KChIPs extends along the entire apical dendrite and into distal dendritic arbors.

As in the hippocampus and other brain regions, immunoreactivity for KChIP1 and Kv4.3 is concentrated in the somata and dendritic branches of interneurons scattered throughout all cortical laminas (Fig. 7). Immunoreactivity was present in virtually all morphological classes of interneurons, including bipolar, multipolar, and bi-tufted cells, among others. Staining for KChIP1 was concentrated in the perinuclear cytoplasm as well as the dendritic cytoplasm of these interneurons, whereas immunoreactivity for Kv4.3 was most intense in the somatodendritic membrane of these cells. Note that in many of these cells the Kv4.3 staining on somata was much less apparent for Kv4.3 than for KChIP1 (Fig. 7).

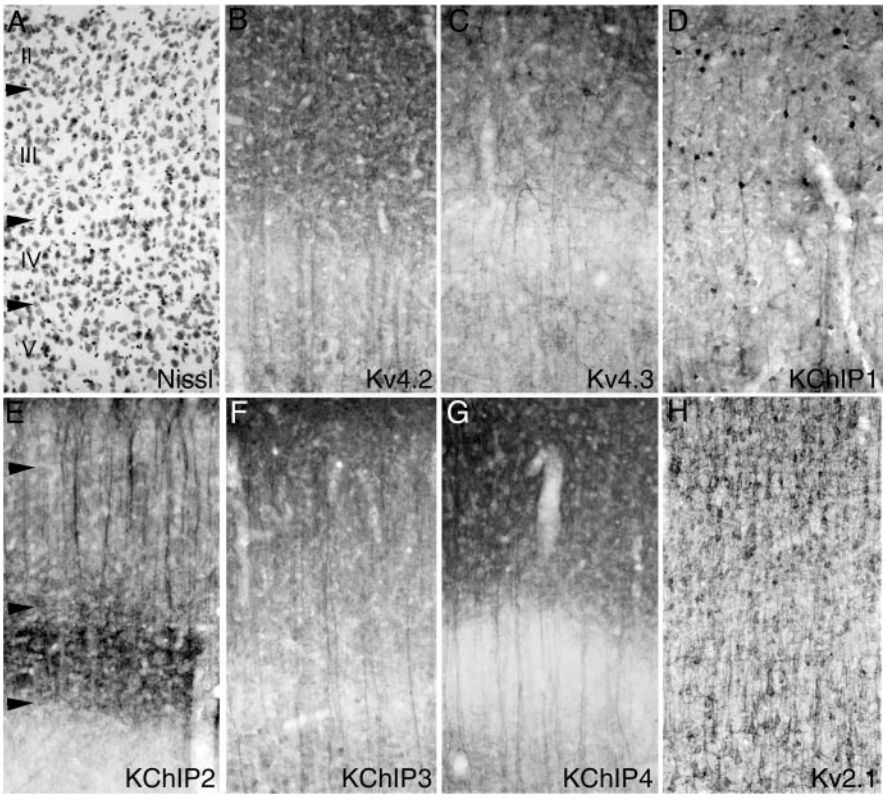

Figure 7. Distribution of Kv4 and KChIP immunoreactivity in the parietotemporal cortex. In neocortical regions such as the parietotemporal cortex (cellular architecture shown by the Nissl stain in *A*), immunoreactivity for Kv4.2 (*B*), Kv4.3 (*C*), and KChIPs 2–4 (*D–G*) is concentrated along the apical dendrites and in the apical dendritic arbors of cortical pyramidal cells. This distribution is particularly striking for Kv4.2, KChIP2, KChIP3, and KChIP4, where the staining lines the large apical dendrites of layer V pyramidal cells as they ascend through layer IV and into more superficial layers and contrasts with the staining pattern for Kv2.1 (*H*), which is limited to the somata and proximal dendritic branches of cortical neurons. As in the hippocampal formation, immunoreactivity for Kv4.3 and KChIP1 is concentrated in the somata and dendrites of cortical interneurons. These interneurons are multipolar, bipolar and fusiform in shape, and are scattered throughout all cortical layers.

Striatum

The pattern of immunoreactivity for Kv4 α subunits and KChIPs in the caudate/putamen is shown in Figure 8. In this brain region, immunoreactivity for Kv4.2, Kv4.3, KChIP2, KChIP3, and KChIP4 is concentrated in the neuropil, where the staining is likely to be associated with the somata and dendrites of striatal projection neurons. However, immunoreactivity for Kv4.2 and KChIP2 in the striatal neuropil is so dense that it is difficult to attribute the staining to a specific cell type or subcellular domain. In contrast to this, immunoreactivity for Kv4.3 and KChIP1 is clearly visible in medium to large-sized multipolar striatal interneurons. Based on the size, distribution, and morphology of these cells, they are likely to represent the somatostatin- and/or neuropeptide Y-containing interneurons. However, detailed analyses using labeling with these specific markers is necessary for a conclusive identification of these immunoreactive cells. Interestingly, immunoreactivity of KChIP4 is concentrated in very large multipolar interneurons (Fig. 8*F*). Based on their size and dendritic morphology, these KChIP4-positive cells are likely to be large cholinergic interneurons that have large A-type currents (Song et al., 1998), although conclusive double-labeling experiments were not performed.

Colocalization of Kv4 and KChIP immunoreactivity

As described above, in many cell types and brain regions, there is clear correspondence and overlap in the distribution of Kv4 and KChIP immunoreactivity. To determine whether and where individual Kv4 α subunits and KChIP isoforms are colocalized within the same cell, we performed double-label immunofluorescence analyses and examined the staining patterns by laser scanning confocal microscopy. Although overlap of immunofluorescence signals indicates that the two target antigens are present within the same cell and subcellular domain, we cannot conclude from this type of analysis that the antigens are coassociated. Thus, these data should be interpreted as suggestive, indicating sites where it is likely that two channel subunits form a channel complex. Our ability to perform these colocalization analyses were limited by the availability of mAbs having compatible isotypes; however, because we initiated our efforts to generate Kv4- and KChIP-specific antibodies with the aim of performing double-label immunofluorescence studies, we were able to select antibody reagents that met our strict selectivity criteria for immunohistochemistry and also satisfied our requirement of isotype compatibility for double-label immunofluorescence.

Representative confocal images showing colocalization of Kv4 and KChIP isoforms are shown in Figure 9. As described above, in many brain regions, immunoreactivity for KChIP1 and Kv4.3 is

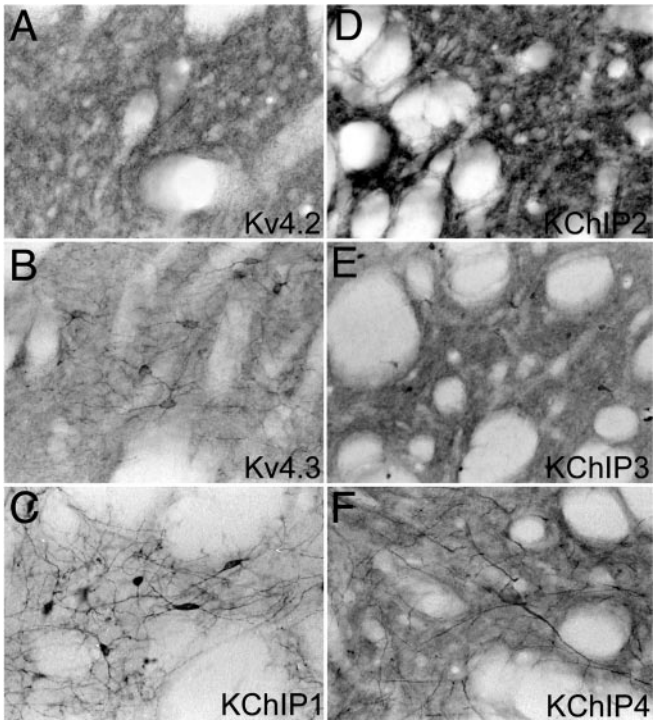

Figure 8. Localization of Kv4 α subunits and KChIPs in the striatum. In the striatal neuropil, there is a very high density of immunoreactivity for Kv4.2 (*A*) and KChIP2 (*D*) and a lower density of immunoreactivity for Kv4.3 (*B*) and KChIPs 3 (*E*) and 4 (*F*). Immunoreactivity for Kv4.3 and KChIP1 (*C*) is concentrated in what appear to be medium-sized striatal interneurons, whereas immunoreactivity for KChIP4 can be observed in very large, multipolar interneurons.

observed in interneurons. As shown in Figure 9, *A–C*, in many, but not all, of these interneurons, Kv4.3 and KChIP1 are colocalized. However, in these interneurons, there is a high density of immunoreactivity for KChIP1 in the perinuclear cytoplasm, as predicted from studies in heterologous cells (Shibata et al., 2003), but no detectable cytoplasmic staining for Kv4.3. Instead, the immunoreactivity for Kv4.3 is predominantly concentrated along the somatodendritic membrane, and here there is also a high density of staining for KChIP1. It is important to point out that in the hippocampus, neocortex, and striatum, virtually all of the cells in which Kv4.3 and KChIP1 are colocalized are interneurons, based on both morphology, density, and location and staining with immunohistochemical markers (supplemental material, available at www.jneurosci.org). In the hippocampus, virtually every Kv4.3-positive cell also expresses KChIP1, and vice versa. Figure 9, *D–F*, also shows colocalization of Kv4.2 with KChIP4 in the dendritic arbors of layer II neurons in the posterior cingulate cortex, in the apical and basal dendrites of CA1 pyramidal cells, and in the glomeruli formed by the dendrites of cerebellar granule cells. In these regions, there is very tight overlap in the patterns of immunofluorescence for Kv4.2 and KChIP4, and it is important to point out that in many of the cells in which colocalization of Kv4.2 with KChIP4 (and KChIP2) was observed are excitatory glutamatergic projection neurons.

Coimmunoprecipitation analyses

The immunohistochemical and immunofluorescence data described above indicate that Kv4.2, Kv4.3, and the four KChIP isoforms show tight overlap in their regional and subcellular distribution across several brain regions but that there is preferential codistribution of Kv4.2 with KChIPs 2, 3, and 4 and preferential codistribution of Kv4.3 with KChIP1. To determine that these channel subunits are not only codistributed but are also coassociated in brain Kv channel complexes, we performed reciprocal coimmunoprecipitation analyses on detergent extracts of rat hippocampal membranes. Because the molecular mass of individual KChIP isoforms and their mobility on SDS-PAGE gels corresponds closely to that for the light chain of IgG, it was not possible to obtain clean, clear, and interpretable results from immunoprecipitation analyses when we used the purified mAbs described above for both immunoprecipitation and immunoblotting. Thus, for coimmunoprecipitation studies, we used affinity-purified rabbit polyclonal antibodies for immunoprecipitation and the purified mAbs to detect associated proteins via immunoblotting. As such, we were limited in the repertoire of available subtype-specific antibodies for the immunoprecipitation reactions. Moreover, the propensity of Kv4.2 to aggregate (Sheng et al., 1993; Shibata et al., 2003) limited the quantitative interpretation of these data. However, as shown in Figure 10, immunoprecipitation reactions performed using an affinity-purified anti-KChIP antibody that recognizes all known KChIP isoforms yielded strong coimmunoprecipitation of Kv4.2 but not Kv2.1 and, as expected, yielded strong immunoprecipitation of each KChIP (1–3) polypeptide analyzed. Immunoprecipitation reactions performed using an affinity-purified antibody against Kv4.2 yielded coimmunoprecipitation of each KChIP isoform. Interestingly, the anti-Kv4.2 antibody also coimmunoprecipitated Kv4.3 (but not Kv2.1), suggesting that Kv4.2 and Kv4.3 may be present in heteromeric Kv4 complexes in

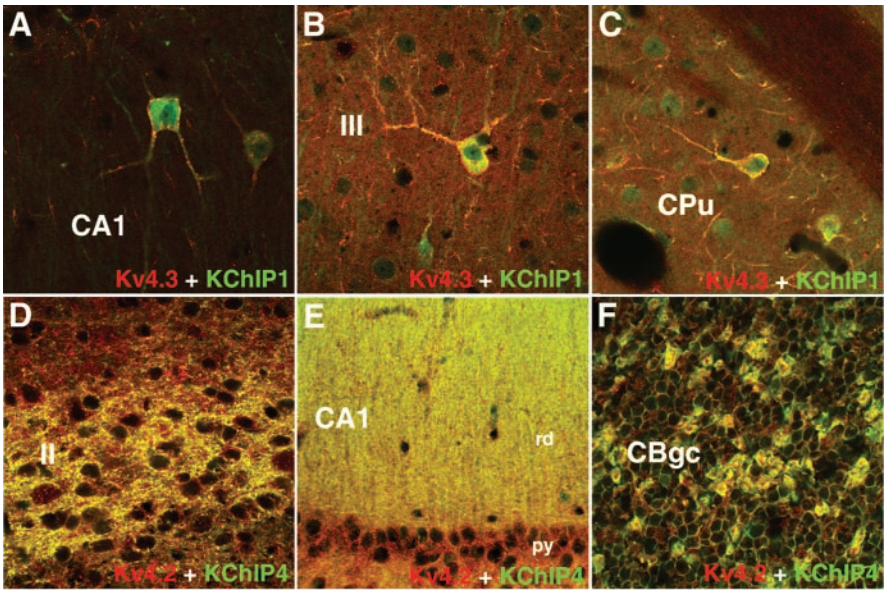

Figure 9. Confocal images showing colocalization of Kv4 and KChIP immunoreactivity. These confocal images show that Kv4.3 (red) and KChIP1 (green) tend to be colocalized in the somatodendritic membranes of hippocampal (*A*), neocortical (*B*), and striatal (*C*) presumed inhibitory interneurons, whereas Kv4.2 (red) and KChIP4 (green) tend to be colocalized in the somatodendritic membranes of presumed excitatory neurons, in the posterior cingulate cortex (*D*), hippocampus (*E*), and cerebellar granule cell layer (*F*).

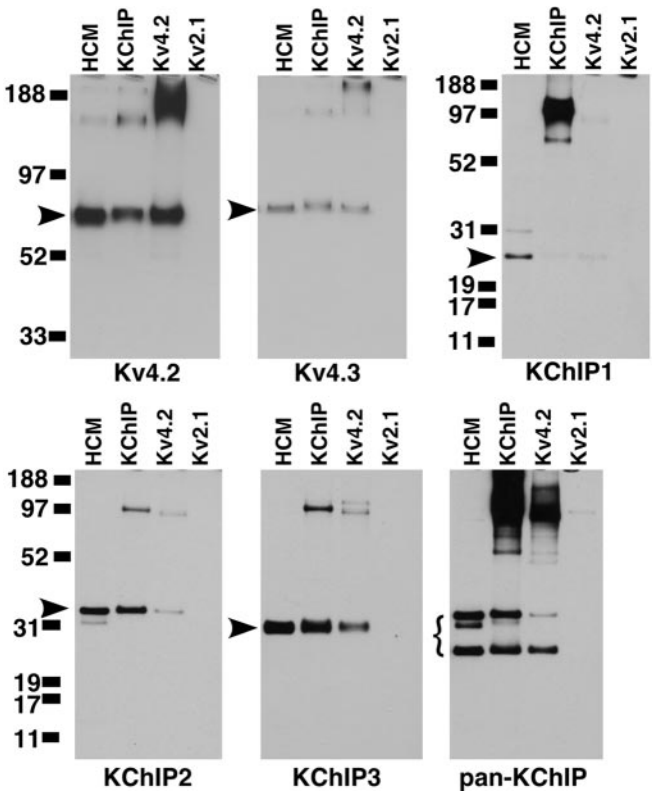

Figure 10. Heteromeric Kv4 and KChIP channel complexes in rat hippocampus. Immunoprecipitation reactions were performed on detergent extracts of adult rat hippocampal membranes (HCM) with the indicated rabbit polyclonal antibodies (anti-KChIP, anti-Kv4.2, or anti-Kv2.1). Aliquots of the HCM detergent extract and of the products of the immunoprecipitation reactions were size fractionated by 4–12% (Kv4 blots) or 10% (KChIP blots) SDS-PAGE. The samples were then transferred to nitrocellulose and probed with mouse mAbs as indicated below each blot panel. Bound antibody was detected by ECL/autoradiography. The arrows or brackets to left of the panels highlight the band resulting from specific detection of the antigen listed below each panel. The numbers to left of the panels refer to electrophoretic mobility of molecular weight standards.

regions in which Kv4.2/Kv4.3 colocalization is observed (e.g., hippocampal dentate granule cells and CA3 pyramidal cell dendrites, glomeruli of cerebellar granule neurons). Taken together, these analyses confirm that Kv4.2 and Kv4.3 are coassociated with KChIP isoforms in rat brain membranes and that the KChIPs are tightly associated with Kv4 α subunits in rat brain Kv channel complexes.

Discussion

Here, we generated and characterized mAbs against Kv4.2, Kv4.3, and KChIPs 1–4 that were used in immunohistochemical and immunoprecipitation analyses of rat brain Kv4 channel complexes. We did not analyze Kv4.1 because specific antibodies were not available. In general, KChIPs 2, 3, and 4 colocalize with Kv4.2 in excitatory neurons including cortical and hippocampal CA1 pyramidal cells, and KChIP1 and Kv4.3 colocalize in inhibitory interneurons throughout the cortex and hippocampus and in striatal interneurons. However, this general inverse relationship between Kv4.2 and Kv4.3, as noted in previous mRNA analyses (Song et al., 1998; Tkatch et al., 2000; Liss et al., 2001; Lien et al., 2002), does not hold for all cell types, in that hippocampal dentate granule and CA3 pyramidal cells and cerebellar granule cells express high levels of colocalized Kv4.2 and Kv4.3. Coimmunoprecipitation analysis in detergent-solubilized hippocampal membranes revealed that all four KChIPs coassociate with Kv4 α subunits in hippocampal membranes, confirming that the KChIPs are tightly associated with Kv4 α subunits in native brain A-type channel complexes.

Although our data confirm that each of the anti-KChIP mAbs described here are specific for their respective antigen, it is important to note that alternatively spliced isoforms of each KChIP polypeptide have been reported (An et al., 2000; Bahring et al., 2001; Decher et al., 2001; Liss et al., 2001; Morohashi et al., 2002; Patel et al., 2002; Boland et al., 2003). Most of the alternative splicing occurs within the variable N termini; a smaller number of splice variants have been reported that contain insertions or deletions within the C-terminal "core" domain. As part of our antibody characterization efforts, we expressed N-terminal truncation mutants of each KChIP polypeptide (An et al., 2000; Holmqvist et al., 2002) in COS cells and tested each mAb for reactivity against the core domain by immunofluorescence. Using this approach, we determined that the epitope for each of the anti-KChIP mAbs maps within the conserved 185 amino acid core domain. Because of this, the staining patterns described here reflect the distribution of all possible N-terminal splice forms for each individual KChIP family member. This point must be considered in interpreting the immunohistochemical staining described here because the specific contribution of KChIP expression to the phenotype of Kv4-mediated currents is likely to depend on the specific splice variant that is expressed (Boland et al., 2003; Decher et al., 2004; Patel et al., 2004). This is especially critical for KChIP4, for which the "KChIP4a" splice variant profoundly slows the kinetics of Kv4 inactivation, but the "KChIP4ap" variant does not (Holmqvist et al., 2002). Although immunohistochemical localization of individual KChIP splice forms will require generation of variant-specific antibodies, valuable information about the contribution of individual KChIP splice variants to Kv4 currents in native cells can also be gained from single-cell analyses of KChIP isoform expression (Liss et al., 2001).

The protein we identified as KChIP3 (An et al., 2000) was identified independently as DREAM, a Ca^{2+}-dependent transcriptional repressor (Carrion et al., 1999), and calsenilin, a presenilin interacting protein (Buxbaum et al., 1999). Recently, Zaidi et al. (2002) described the distribution of calsenilin immunoreactivity in mouse brain, using a rabbit polyclonal antibody raised against a full-length calsenilin/KChIP3 fusion protein, which is likely to cross-react with other KChIP family members. Their immunoblot data strongly support this contention because in mouse brain membranes their antibody detects several bands in the 25–35 kDa range, corresponding to the predicted molecular masses of other KChIP family members (Zaidi et al., 2002). Interestingly, neither the polyclonal antibody used by Zaidi et al. (2002) nor our KChIP3-specific mAb exhibit staining in the nucleus of neurons or glial cells, which might be expected for a Ca^{2+}-dependent regulator of transcription (Carrion et al., 1999; Cheng et al., 2002). The remarkable correspondence between Kv4.2 (Sheng et al., 1992; present study) and KChIP3 (Zaidi et al., 2002; present study) localization suggests that the preferred binding partner for KChIP3 in neurons is Kv4.2, raising questions as to whether KChIP3 in native cells is truly the multifunctional protein suggested by studies in heterologous expression systems.

Somatodendritic A-currents have been studied most extensively by patch clamp in hippocampal pyramidal cells and in the large layer V pyramidal neurons in the motor and somatosensory cortex (Wu and Barish, 1992; Hoffman et al., 1997; Hoffman and Johnston, 1998; Golding et al., 1999; Bekkers, 2000a,b; Johnston et al., 2000; Korngreen and Sakmann, 2000; Storm, 2000). In CA1

pyramidal cells, A-type currents play a critical role in synaptic integration and plasticity by controlling subthreshold excitation and the amplitude of back-propagating action potentials (Hoffman et al., 1997; Johnston et al., 2000). In these cells, the density of A-type currents on the trunk of the apical dendrite increases dramatically with distance from the pyramidal cell soma (Hoffman et al., 1997). We did not observe a striking gradient in the intensity of Kv4.2, KChIP2, or KChIP4 immunoreactivity across the stratum radiatum of CA1 using immunoperoxidase staining, although a striking gradient was observed across dendrites of dentate granule cells in the molecular layer of the denate gyrus. Confocal analysis of sections with double immunofluorescence staining for Kv4.2 and KChIP4 (Fig. 9*E*) or Kv4.2 and PSD-95 (supplemental material, available at www.jneurosci.org) revealed only a subtle increase in the density of Kv4.2 immunoreactivity in the superficial third of the stratum radiatum. Unlike in the neocortex (see below), the extremely close packing of CA1 pyramidal cells precludes detailed immunocytochemical analyses of individual apical dendrites required for conclusive correlations with electrophysiological studies. Moreover, our experiments label Kv4.2 not only on the main trunk of the apical dendrites accessible by patch clamp but also each branch and collateral in the entire, and very complex, intertwining dendritic trees of the densely packed CA1 pyramidal neurons. We are also visualizing both intracellular and surface pools of Kv4.2 in our detergent-permeabilized sections. Finally, dynamic modulation of dendritic Kv4 channel activity by phosphorylation (Hoffman and Johnston, 1998; Varga et al., 2000; Schrader et al., 2002; Frick et al., 2004) may lead to inconsistencies between the density of channel protein and functional channels.

Two striking findings in the present study are that in CA1–CA3, there is an abrupt decrease in the density of Kv4.2 (and KChIP2, 3, and 4) at the transition from the stratum radiatum to the stratum moleculare and that there is little or no Kv4.3 immunoreactivity in CA1 pyramidal cells but a high density of Kv4.3 (with Kv4.2) immunoreactivity in CA3 pyramids. The very low density of Kv4.3 immunoreactivity in CA1 compared with CA3 pyramidal cells suggest that in CA1 pyramidal cells, the majority of A-type channel complexes are homomeric Kv4.2 channels. To our knowledge, there is little published data exploring the detailed biophysical properties of heteromeric channels formed by coexpression of Kv4.2 and Kv4.3 or concatenated α subunits (but see Guo et al., 2002). Nevertheless, the dramatic change in Kv4 α subunit expression in these adjacent hippocampal subfields is intriguing. The drop-off of Kv4 and KChIP immunoreactivity in the stratum moleculare suggests a very low density of Kv4-mediated A-type current in very distal dendrites of CA pyramidal cells.

Neocortical layer V pyramidal cells differ from hippocampal CA1 pyramidal cells in that they do not express a gradient of A-current along the apical dendrite and in having a much lower density of dendritic A-type current (Hoffman et al., 1997; Bekkers, 2000a,b; Korngreen and Sakmann, 2000). This suggests that dendritic A-current does not exert as dominant an influence in cortical pyramidal cells as it does in CA1 (Storm, 2000). Here, we observed that immunoreactivity for Kv4.2 and KChIPs 2, 3, and 4 can be followed along the entire apical dendrite of cortical layer V pyramidal cells and that there is a fairly uniform density of immunoreactivity along the dendritic shaft. It is important to note that Kv4.2 and KChIP immunoreactivity can be followed all the way into the most distal dendritic branches and the apical dendritic tufts of cortical pyramidal cells. The presence of Kv4 immunoreactivity in the most distal dendritic regions indicates that these channels may modulate excitatory input along the entire dendrite and that in neocortical pyramidal cells, A-type currents are not as compartmentalized within the dendrite as they are in hippocampal CA pyramids.

Although KChIPs are clearly a component of the Kv4 modulatory factors encoded in brain mRNA (Nadal et al., 2001), another factor that accelerates Kv4 inactivation has been identified as the CD26-like dipeptidyl-peptidase dipeptidyl aminopeptidase-like protein (DPPX) (Nadal et al., 2003). Coexpression of Kv4 α subunits with KChIPs and DPPX in heterologous cells gives rise to currents that recapitulate the features of native A-type currents, indicating that native brain Kv4 channels are likely to be formed as complexes of all three proteins. Future studies are needed to explore the relative contributions of DPPX and KChIPs to the formation of A-type currents in native neurons.

References

An WF, Bowlby MR, Betty M, Cao J, Ling HP, Mendoza G, Hinson JW, Mattsson KI, Strassle BW, Trimmer JS, Rhodes KJ (2000) Modulation of A-type potassium channels by a family of calcium sensors. Nature 403:553–556.

Bahring R, Dannenberg J, Peters HC, Leicher T, Pongs O, Isbrandt D (2001) Conserved Kv4 N-terminal domain critical for effects of Kv channel-interacting protein 2.2 on channel expression and gating. J Biol Chem 276:23888–23894.

Baldwin TJ, Tsaur ML, Lopez GA, Jan YN (1991) Characterization of a mammalian cDNA for an inactivating voltage-sensitive K^+ channel. Neuron 7:471–483.

Bekele-Arcuri Z, Matos MF, Manganas L, Strassle BW, Monaghan MM, Rhodes KJ, Trimmer JS (1996) Generation and characterization of subtype-specific monoclonal antibodies to K^+ channel α- and β-subunit polypeptides. Neuropharmacology 35:851–865.

Bekkers JM (2000a) Properties of voltage-gated potassium currents in nucleated patches from large layer 5 cortical pyramidal neurons of the rat. J Physiol (Lond) 525:593–609.

Bekkers JM (2000b) Distribution and activation of voltage-gated potassium channels in cell-attached and outside-out patches from large layer 5 cortical pyramidal neurons of the rat. J Physiol (Lond) 525:611–620.

Boland LM, Jiang M, Lee SY, Fahrenkrug SC, Harnett MT, O'Grady SM (2003) Functional properties of a brain-specific N-terminally spliced modulator of Kv4 channels. Am J Physiol Cell Physiol 285:C161–C170.

Buxbaum JD, Choi EK, Luo Y, Lilliehook C, Crowley AC, Merriam DE, Wasco W (1998) Calsenilin: a calcium-binding protein that interacts with the presenilins and regulates the levels of a presenilin fragment. Nat Med 4:1177–1181.

Carrion AM, Link WA, Ledo F, Mellstrom B, Naranjo JR (1999) DREAM is a Ca^{2+}-regulated transcriptional repressor. Nature 398:80–84.

Chabala LD, Bakry N, Covarrubias M (1993) Low molecular weight poly(A)+ mRNA species encode factors that modulate gating of a non-Shaker A-type K^+ channel. J Gen Physiol 102:713–728.

Cheng HY, Pitcher GM, Laviolette SR, Whishaw IQ, Tong KI, Kockeritz LK, Wada T, Joza NA, Crackower M, Goncalves J, Sarosi I, Woodgett JR, Oliveira-dos-Santos AJ, Ikura M, van der Kooy D, Salter MW, Penninger JM (2002) DREAM is a critical transcriptional repressor for pain modulation. Cell 108:31–43.

Decher N, Uyguner O, Scherer CR, Karaman B, Yuksel-Apak M, Busch AE, Steinmeyer K, Wollnik B (2001) hKChIP2 is a functional modifier of hKv4.3 potassium channels: cloning and expression of a short hKChIP2 splice variant. Cardiovasc Res 52:255–264.

Decher N, Barth AS, Gonzalez T, Steinmeyer K, Sanguinetti MC (2004) Novel KChIP2 isoforms increase functional diversity of transient outward potassium currents. J Physiol (Lond) 557:761–772.

Du J, Tao-Cheng JH, Zerfas P, McBain CJ (1998) The K+ channel, Kv2.1, is apposed to astrocytic processes and is associated with inhibitory postsynaptic membranes in hippocampal and cortical principal neurons and inhibitory interneurons. Neuroscience 84:37–48.

Frick A, Magee J, Johnston D (2004) LTP is accompanied by an enhanced

local excitability of pyramidal neuron dendrites. Nat Neurosci 7:126–135.

Golding NL, Jung H, Mickus T, Spruston N (1999) Dendritic calcium spike initiation and repolarization are controlled by distinct potassium channel subtypes in CA1 pyramidal neurons. J Neurosci 19:8789–8798.

Guo W, Li H, Aimond F, Johns DC, Rhodes KJ, Trimmer JS, Nerbonne JM (2002) Role of heteromultimers in the generation of myocardial transient outward K+ currents. Circ Res 90:586–593.

Gutman GA, Chandy KG, Adelman JP, Aiyar J, Bayliss DA, Clapham DE, Covarriubias M, Desir GV, Furuichi K, Ganetzky B, Garcia ML, Grissmer S, Jan LY, Karschin A, Kim D, Kuperschmidt S, Kurachi Y, Lazdunski M, Lesage F, Lester HA, et al. (2003) International Union of Pharmacology. XLI. Compendium of voltage-gated ion channels: potassium channels. Pharmacol Rev 55:583–586.

Hoffman DA, Johnston D (1998) Downregulation of transient K^+ channels in dendrites of hippocampal CA1 pyramidal neurons by activation of PKA and PKC. J Neurosci 18:3521–3528.

Hoffman DA, Magee JC, Colbert CM, Johnston D (1997) K^+ channel regulation of signal propagation in dendrites of hippocampal pyramidal neurons. Nature 387:869–875.

Holmqvist MH, Cao J, Knoppers MH, Jurman ME, Distefano PS, Rhodes KJ, Xie Y, An WF (2001) Kinetic modulation of Kv4-mediated A-current by arachidonic acid is dependent on potassium channel interacting proteins. J Neurosci 21:4154–4161.

Holmqvist MH, Cao J, Hernandez-Pineda R, Jacobson MD, Carroll KI, Sung MA, Betty M, Ge P, Gilbride KJ, Brown ME, Jurman ME, Lawson D, Silos-Santiago I, Xie Y, Covarrubias M, Rhodes KJ, Distefano PS, An WF (2002) Elimination of fast inactivation in Kv4 A-type potassium channels by an auxiliary subunit domain. Proc Natl Acad Sci USA 99:1035–1040.

Johnston D, Hoffman DA, Magee JC, Poolos NP, Watanabe S, Colbert CM, Migliore M (2000) Dendritic potassium channels in hippocampal pyramidal neurons. J Physiol (Lond) 525:75–81.

Johnston D, Christie BR, Frick A, Gray R, Hoffman DA, Schexnayder LK, Watanabe S, Yuan LL (2003) Active dendrites, potassium channels and synaptic plasticity. Philos Trans R Soc Lond B Biol Sci 358:667–674.

Kim LA, Furst J, Butler MH, Xu S, Grigorieff N, Goldstein SA (2004a) Ito channels are octomeric complexes with four subunits of each Kv4.2 and K+ channel-interacting protein 2. J Biol Chem 279:5549–5554.

Kim LA, Furst J, Gutierrez D, Butler MH, Xu S, Goldstein SA, Grigorieff N (2004b) Three-dimensional structure of I(to); Kv4.2-KChIP2 ion channels by electron microscopy at 21 Angstrom resolution. Neuron 41:513–519.

Korngreen A, Sakmann B (2000) Voltage-gated K^+ channels in layer 5 neocortical pyramidal neurones from young rats: subtypes and gradients. J Physiol (Lond) 525:621–639.

Lien CC, Martina M, Schultz JH, Ehmke H, Jonas P (2002) Gating, modulation and subunit composition of voltage-gated K(+) channels in dendritic inhibitory interneurons of rat hippocampus. J Neurophysiol 538:405–409.

Liss B, Franz O, Sewing S, Bruns R, Neuhoff H, Roeper J (2001) Tuning pacemaker frequency of individual dopaminergic neurons by Kv4.3L and KChip3.1 transcription. EMBO J 20:5715–5724.

Maletic-Savatic M, Lenn NJ, Trimmer JS (1995) Differential spatiotemporal expression of K^+ channel polypeptides in rat hippocampal neurons developing *in situ* and *in vitro*. J Neurosci 15:3840–3851.

Monaghan MM, Trimmer JS, Rhodes KJ (2001) Experimental localization of Kv1 family voltage-gated K^+ channel α and β subunits in rat hippocampal formation. J Neurosci 21:5973–5983.

Morohashi Y, Hatano N, Ohya S, Takikawa R, Watabiki T, Takasugi N, Imaizumi Y, Tomita T, Iwatsubo T (2002) Molecular cloning and characterization of CALP/KChIP4, a novel EF-hand protein interacting with presenilin 2 and voltage-gated potassium channel subunit Kv4. J Biol Chem 277:14965–14975.

Nadal MS, Amarillo Y, Vega-Saenz de Miera E, Rudy B (2001) Evidence for the presence of a novel Kv4-mediated A-type K(+) channel-modifying factor. J Physiol (Lond) 537:801–809.

Nadal MS, Ozaita A, Amarillo Y, de Miera EV, Ma Y, Mo W, Goldberg EM, Misumi Y, Ikehara Y, Neubert TA, Rudy B (2003) The CD26-related dipeptidyl aminopeptidase-like protein DPPX is a critical component of neuronal A-type K^+ channels. Neuron 37:449–461.

Nakamura TY, Coetzee WA, Vega-Saenz De Miera E, Artman M, Rudy B (1997) Modulation of Kv4 channels, key components of rat ventricular transient outward K^+ current, by PKC. Am J Physiol 273:H1775–H1786.

Patel SP, Campbell DL, Morales MJ, Strauss HC (2002) Heterogeneous expression of KChIP2 isoforms in the ferret heart. J Physiol (Lond) 15:649–656.

Patel SP, Parai R, Parai R, Campbell DL (2004) Regulation of Kv4.3 voltage-dependent gating kinetics by KChIP2 isoforms. J Physiol (Lond) 557:19–41.

Rhodes KJ, Keilbaugh SA, Barrezueta NX, Lopez KL, Trimmer JS (1995) Association and colocalization of K^+ channel α- and β-subunit polypeptides in rat brain. J Neurosci 15:5360–5371.

Rhodes KJ, Monaghan MM, Barrezueta NX, Nawoschik S, Bekele-Arcuri Z, Matos M, Nakahira K, Schechter LE, Trimmer JS (1996) Voltage-gated K^+ channel β-subunits: expression and distribution of Kvβ1 and Kvβ2 in adult rat brain. J Neurosci 16:4846–4860.

Rhodes KJ, Strassle BW, Monaghan MM, Bekele-Arcuri Z, Matos MF, Trimmer JS (1997) Association and colocalization of Kvβ1 and Kvβ2 with Kv1 α-subunits in mammalian brain K^+ channel complexes. J Neurosci 17:8246–8258.

Rudy B, Hoger JH, Lester HA, Davidson N (1988) At least two mRNA species contribute to the properties of rat brain A-type potassium channels expressed in *Xenopus* oocytes. Neuron 1:649–658.

Scannevin RH, Murakoshi H, Rhodes KJ, Trimmer JS (1996) Identification of a cytoplasmic domain important in the polarized expression and clustering of the Kv2.1 K+ channel. J Cell Biol 135:1619–1632.

Scannevin RH, Wang K, Jow F, Megules J, Kopsco DC, Edris W, Carroll KC, Lu Q, Xu W, Xu Z, Katz AH, Olland S, Lin L, Taylor M, Stahl M, Malakian K, Somers W, Mosyak L, Bowlby MR, Chanda P, Rhodes KJ (2004) Two N-terminal domains of Kv4 K(+) channels regulate binding to and modulation by KChIP1. Neuron 19:587–598.

Schrader LA, Anderson AE, Mayne A, Pfaffinger PJ, Sweatt JD (2002) PKA modulation of Kv4.2-encoded A-type potassium channels requires formation of a supramolecular complex. J Neurosci 22:10123–10133.

Serôdio P, Rudy B (1998) Differential expression of Kv4 K^+ channel subunits mediating subthreshold transient K^+ (A-type) currents in rat brain. J Neurophysiol 79:1081–1091.

Serôdio P, Kentros C, Rudy B (1994) Identification of molecular components of A-type channels activating at subthreshold potentials. J Neurophysiol 72:1516–1529.

Serôdio P, Vega-Saenz de Miera E, Rudy B (1996) Cloning of a novel component of A-type K^+ channels operating at subthreshold potentials with unique expression in heart and brain. J Neurophysiol 75:2174–2179.

Sheng M, Tsaur ML, Jan YN, Jan LY (1992) Subcellular segregation of two A-type K^+ channel proteins in rat central neurons. Neuron 9:271–284.

Sheng M, Liao YJ, Jan YN, Jan LY (1993) Presynaptic A-current based on heteromultimeric K+ channels detected in vivo. Nature 365:72–75.

Shibata R, Misonou H, Campomanes CR, Anderson AE, Schrader LA, Doliveira LC, Carroll KI, Sweatt JD, Rhodes KJ, Trimmer JS (2003) A fundamental role for KChIPs in determining the molecular properties and trafficking of Kv4.2 potassium channels. J Biol Chem 278:36445–36454.

Song WJ, Tkatch T, Baranauskas G, Ichinohe N, Kitai ST, Surmeier DJ (1998) Somatodendritic depolarization-activated potassium currents in rat neostriatal cholinergic interneurons are predominantly of the A type and attributable to coexpression of Kv4.2 and Kv4.1 subunits. J Neurosci 18:3124–3137.

Storm JF (2000) K($^+$) channels and their distribution in large cortical pyramidal neurones. J Physiol (Lond) 525:565–566.

Tago H, Kimura H, Maeda T (1986) Visualization of detailed acetylcholinesterase fiber and neuron staining in rat brain by a sensitive histochemical procedure. J Histochem Cytochem 34:1431–1438.

Tekirian TL, Merriam DE, Marshansky V, Miller J, Crowley AC, Chan H, Ausiello D, Brown D, Buxbaum JD, Xia W, Wasco W (2001) Subcellular localization of presenilin 2 endoproteolytic C-terminal fragments. Brain Res Mol Brain Res 96:14–20.

Tkatch T, Baranauskas G, Surmeier DJ (2000) Kv4.2 mRNA abundance and A-type K(+) current amplitude are linearly related in basal ganglia and basal forebrain neurons. J Neurosci 20:579–588.

Trimmer JS (1991) Immunological identification and characterization of a delayed rectifier K^+ channel polypeptide in rat brain. Proc Natl Acad Sci USA 88:10764–10768.

Trimmer JS, Rhodes KJ (2004) Localization of voltage-gated ion channels in mammalian brain. Annu Rev Physiol 66:477–519.

Trimmer JS, Trowbridge IS, Vacquier VD (1985) Monoclonal antibody to a membrane glycoprotein inhibits the acrosome reaction and associated Ca^{2+} and H^+ fluxes of sea urchin sperm. Cell 40:697–703.

Tsaur ML, Chou CC, Shih YH, Wang HL (1997) Cloning, expression and CNS distribution of Kv4.3, an A-type K+ channel alpha subunit. FEBS Lett 400:215–220.

Varga AW, Anderson AE, Adams JP, Vogel H, Sweatt JD (2000) Input-specific immunolocalization of differentially phosphorylated Kv4.2 in the mouse brain. Learn Mem 7:321–332.

Wu RL, Barish ME (1992) Two pharmacologically and kinetically distinct transient potassium currents in cultured embryonic mouse hippocampal neurons. J Neurosci 12:2235–2246.

Zaidi NF, Berezovska O, Choi EK, Miller JS, Chan H, Lilliehook C, Hyman BT, Buxbaum JD, Wasco W (2002) Biochemical and immunocytochemical characterization of calsenilin in mouse brain. Neuroscience 114:247–263.

Zhou W, Qian Y, Kunjilwar K, Pfaffinger PJ, Choe S (2004) Structural insights into the functional interaction of KChIP1 with Shal-type K(+) channels. Neuron 41:573–586.